MedChemComm

PEGylated Solid Lipid Nanoparticles: Design, methotrexate loading and biological evaluation in animal models

Journal:	*MedChemComm*
Manuscript ID:	MD-CAR-03-2015-000104.R1
Article Type:	Concise Article
Date Submitted by the Author:	21-May-2015
Complete List of Authors:	Kakkar, Dipti; INMAS, DCRS dumoga, shweta; INMAS, Kumar, Rohit; INMAS, Chuttani, Krishna; INMAS, Mishra, A K; INMAS,

Journal Name

RSCPublishing

ARTICLE

PEGylated Solid Lipid Nanoparticles: Design, methotrexate loading and biological evaluation in animal models

Cite this: DOI: 10.1039/x0xx00000x

Received 00th January 2012,
Accepted 00th January 2012

DOI: 10.1039/x0xx00000x

www.rsc.org/

Dipti Kakkar*, Shweta Dumoga, Rohit Kumar, Krishna Chuttani and Anil Kumar Mishra*

Abstract

Poor bioavailability of chemotherapeutic drugs such as methotrexate(MTX), play a critical role in their success. Solid Lipid nanoparticles(SLNs) have come up as vital therapeutic carriers owing to the biocompatible nature of their constituent materials. In this study, a nanoparticulate system, consisting of a pegylated lipid core of stearic acid has been designed to evaluate its potential for encapsulation and delivery of the chemotherapeutic drug, MTX, which often suffers from poor bioavailability. Stable pegylated SLN formulations of MTX having mean particle size ~130nm(Zeta Potential -34mV) and low polydispersity were prepared and completely characterized by DSC, TEM and AFM. They were found to present almost spherical morphology. These drug loaded formulations were found to have good hemocompatibility as quantified by hemolysis analysis. In vitro drug release studies at acidic pH(5.5) and physiological pH(7.4)revealed a power-law mechanism of release MTX from the SLNs. These MTX loaded formulations have been evaluated biologically with the help of radiolabeling techniques (with ^{99m}Tc radionuclide). Blood kinetics profile of the ^{99m}Tc radiolabeled pegylated MTX formulations in New Zealand Albino rabbits revealed higher blood circulation times while the biodistribution studies in tumour models(balb/c mice) revealed their efficient tumour uptake as evidenced by SPECT imaging. These studies convey the potential use of these pegylated SLNs based on stearic acid for improving the bioavailability of MTX and they can be expected to be a valuable addition to the array of nanoparticles with potential therapeutic applications.

Introduction

Drug delivery methodologies have traditionally known to gratify locally approachable areas at or near the surface of the human body, generally by the oral, nasal, ocular and tropical modes of administration. However, delivery of drugs to deep-seated internal organs is often challenging as the only access to these organs is through the bloodstream. This route, which is flanked by drawbacks of adverse effects on other parts of the body, poses even more problems in case of drugs with poor or low bioavailability. Therefore, poor bioavailability of several available chemotherapeutic drugs poses a major technical challenge limiting their development to leverage their complete potential in-vivo. In recent years nanotechnology has come up with significant applications in pharmaceutical research to aid in the delivery of such drugs.[1] Solid lipid nanoparticles (SLNs) have become an interesting part of the nanomedicine paraphernalia and are seen as important biocompatible delivery systems for anti-cancer drugs (hydrophobic and hydrophilic), peptides and proteins and gene therapy.[2-5] Moreover, SLNs represent an alternative carrier system to conventional colloidal carriers such as emulsions, liposomes and polymeric micro- and nanoparticles, combining the advantages of traditional systems and avoiding some of their major disadvantages[6] SLN based delivery systems offer the much desired advantages including biocompatibility of the carrier system, controlled release of the entrapped drug, targeting ability, decreased degradation and enhanced bioavailability of the loaded components.[7-9] Their small diameter and narrow particle size distribution that attribute to their excellent physicochemical and biological properties help them play a pivotal role in pharmaceutical applications. Infact, SLNs have scored over other carrier systems like polymeric nanoparticles or liposomes as they prove economical owing to their low-cost excipients and easy scale up options offered by them. It is possible to overcome stability problems e.g. drug leakage or coalescence, often observed for lipid dispersions, by

using particles with a solid lipid matrix. In comparison to liposomes they offer better stability and protection to the entrapped drug as they give little or no access of the inner core of lipid particles to surrounding water. SLNs are known to deliver encapsulated drugs to tumours, however their relative rapid clearance hampers the development of effective carrier systems for anticancer drugs.

Surface association of certain polymers such as the ganglioside GM1 and polyethylene glycol (PEG) have shown to increase the circulation lifetime of conventional SLNs to give sterically stabilized long-circulating SLNs.[10-11] PEG serves to reduce absorption of the immunoproteins and consequently slow down clearance by the MPS by avoiding opsonization.[12] PEG modified SLNs have been reported to enhance/improve the biological half-life and efficacy of the encapsulated drugs, enhance stability, also their transport and absorption through the GI tract.[13-15] Nanocarriers are reported to obtain stealthiness through pegylation which is reported to largely minimize interactions with proteins and enzymes that may jeopardize their own stability, otherwise. Furthermore, PEG reduces the tendency of particles to aggregate by steric stabilization, thereby resulting in formulations with increased stability during storage and application.[16]

Methotrexate (MTX) is an anti-metabolite that works by blocking crucial metabolic pathways essential for cell growth like the synthesis of thymine, required for DNA synthesis during cell growth. It is the most recognized representative in the class of suitable folic acid antagonists being developed as cytotoxic agents. Owing to this, it is found effective against a range of solid tumours including breast, non-hodgkins lymphoma, hodgkins disease, acute lymphocytic leukemia, head and neck cancer, bladder and trophoblastic neoplasms as well as autoimmune diseases.[17] Being an anti-proliferative, it is capable of inducing apoptosis and thereby prevents metastasis of tumour cells. MTX is proven to be a promising anti-tumour agent and its mechanism is associated with its capabilities of inhibiting dihydrofolate reductase (DHFR) resulting in depletion of crucial reduced folates, inhibition of de-novo thymidylate and purine synthesis.[18] Despite its distinctive biological activities, MTX presents low aqueous solubility(0.01mg/mL) and poor bioavailability.[19] Another drawback is the incomplete absorption of the native drug as 80-90% of the administered dose is eliminated unchanged in urine within 24h, after i.v. administration. The 10-20 % of the administered drug that is absorbed, tends to degrade rapidly in blood and present toxicity to normal tissues which are limiting factors to its effectiveness resulting in decreased patient compliance, poor quality of life and significant dose reduction compromising its efficacy and even life-threatening events.[20] Due to this, patients taking MTX are more likely to discontinue therapies because of the adverse effects of medication rather than lack of efficacy. Attempts are on to reduce its toxic dose-related side effects to improvise its clinical application as the major DHFR inhibitor.[21] Given the undesirable pharmacokinetic properties of MTX (short plasma half-life (2-10h), low permeability (C logP=0.53)) accompanied by its high toxicity to normal cells, a nanocarrier /nanodelivery system for MTX represents an attractive prospect to overcome these issues. Encapsulation of MTX in SLNs presents an important strategy for reducing the intrinsic drawbacks of this drug and enhancing its efficacy.

MTX has been reported earlier to be encapsulated in lipids like stearic acid, cetyl alcohol and Compritol 888 by Misra et. al. for psoriasis treatment.[22] MTX loaded stearic acid SLNs, stabilized by soyalecithin and sodium taurodeoxycholate, were prepared by other groups previously, but the entire loaded MTX was found to release within 15h.[23, 24] We have tried to overcome the drawback of quick release in these systems, by preparing pegylated SLNs to harness stealth characteristics to our formulation, thus ensuring retention in systemic circulation and a sustained release of the drug. However, while designing nanocarriers/nanodelivery systems with desirable characteristics, it is imperative to understand the mechanisms by which a carrier retains the drug till it reaches the target site and releases a drug at or near the target organ/tissue, the effects of composition and morphology of the carrier on the drug release kinetics and the eventual clearance of these systems from the physiological system. Also, the rapid clearance of SLNs injected by the i.v. route is still an issue to be dealt with. Therefore, to address these issues, the present study was undertaken to design pegylated stearic acid SLNs to encapsulate MTX for its in-vivo delivery and to evaluate the influence of pegylation on the toxicity and bioavailability of the drug, especially with regard to its tumour uptake and systemic clearance. These MTX-loaded pegylated SLN formulations were evaluated in terms of physicochemical properties and investigated by in-vitro and in-vivo analysis in mice and rabbits, with the help of radiological techniques.

Results

The purpose of this study/work was to develop a biocompatible carrier system for MTX aimed at improving its therapeutic index and reducing its toxicity to tolerable limits. In addition, this work also aimed to compare the behaviour of these drug loaded carrier systems/SLNs when they are pegylated or non-pegylated. The formulation and preparation of stearic acid SLNs was optimized to enable encapsulation of MTX. The lipid concentration, drug: lipid molar ratio and concentration of surfactant are known to have a significant influence on the particle size and drug entrapment efficiency. The optimization of these parameters to attain an effective MTX-loaded SLN formulation and its biological evaluation is presented herein.

Physicochemical characteristics of SLNs

The physicochemical characteristics of SLNs play a crucial role in their successful utilization. Therefore, it is imperative to comprehend the effect of the materials and preparation processes on the properties of SLNs. With this view, the particle size, morphology and thermal behaviour of the prepared SLNs were studied.

The particle size distribution and zeta potential values of all the pegylated and non-pegylated formulations prepared as part of this study are given in Table 1.

The mean particle size of the stearic acid SLNs was found to be in the range of 135nm to 214nm. From the lipid and surfactant variation study, the formulation SA5, which gave a showed unimodal narrow particle size distribution was taken up for the pegylation study [Table 1]. On pegylation the sizes were found to slightly decrease and varied from 154 to 127 nm. This decrease in size has also been reported earlier by Yuan et. al. for similar formulations.[13] PDI describes the dispersion homogeneity and values greater than 0.3 indicate high

heterogeneity. Therefore, formulation SD4 was chosen as an optimal formulation for further drug loading experiments owing to its best combination of optimum particle size and PDI<0.3 [Table 1]. Drug loading of SD4 was carried out at different concentrations of lipid and drug; 0.1:1.0::drug:lipid to 1:1::drug:lipid as shown in Table 2. Formulation PSD4, showed encapsulation efficiency around 70% and drug loading around 22%. The zeta potential values are known to be helpful in predicting the storage stability of colloidal dispersions.[25] In general, it is said that the greater the absolute zeta potential value of a nanoparticulate system better is the stability of the colloidal suspension due to repulsion effect between charged nanoparticles. The absolute zeta potential of this MTX loaded pegylated SLN was more than 30mV which could attribute reasonable stability to the formulation and contribute to the improvement of its surface hydrophilicity. This drug loaded formulation, PSD4, hereafter named M-P-SLN was taken up for further evaluations (Figure 1).

The TEM micrographs revealed that this solvent diffusion process leads to the formation of almost spherical SLNs with a smooth surface even though the use of different concentrations of solvent and surfactant, or the lipid load might influence the surface morphology or size of the particles. The spherical morphology was retained even on drug loading as seen in the TEM images (Figure 2). AFM imaging corroborated the TEM micrographs. However, the dehydration and shrinkage of the particles during the sample processing for TEM and AFM measurement may be the possible reason for the relatively smaller particle size compared to the hydrodynamic size obtained by dynamic light scattering (DLS).

Supercooled melts present in SLN systems describe the phenomenon that lipid crystallization may not occur in a sample although it is stored at a temperature below the melting point of the lipid.[26] As the advantage for SLN drug-carrier system is essentially based on the solid state of the particles, the solidification of the particles after the dilution of the emulsions has to be ensured. For this, the differential scanning calorimetry analysis of the lipid nanoparticles obtained from emulsions stabilized with tween-80 and soyalecithin was carried out. The DSC scans gave vital information regarding the physical properties like crystallinity or amorphous nature of the samples. Figure 3 shows the DSC thermograms of the pegylated stearic acid SLNs, the pure drug (MTX) and the MTX loaded pegylated SLNs. These showed characteristic endothermic peaks. Investigation of the DSC scans for pure MTX showed a sharp melting endotherm at 195.94°C, corresponding to its melting point (185-204°C). The DSC analysis of the MTX loaded SLNs showed an absence of a significant shift in the endothermic peak of MTX (the peak shifted only slightly from 195.94 to 197.07°C), which is an indication of the lack of significant changes in the crystalline state of the drug and hence also an evidence of the presence of the drug in the carrier system. The encapsulation of the drug is also substantiated by the huge decrease in the enthalpy of the free drug from 250.27mcal to 43.33mcal in case of the MTX loaded formulation. Also, the thermograms of the pegylated formulation showed the characteristic peak of the carrier matrix around 51°C (Tm of PEG ~55°C), along with the drug endothermic melting peak, indicating that the drug remained in the crystalline state in the pegylated dispersion as well.

In vitro Drug Release

The physical state of the particles holds importance from the biopharmaceutical point of view. It is possible to overcome stability problems e.g. drug leakage or coalescence, often observed for lipid dispersions, by using particles with a solid lipid matrix. Also, drug release from solid matrix is supposed to be degradation-controlled and thus slower than diffusion-controlled release from emulsions. In order to investigate further, the in-vitro release profiles were drawn by representing the percentage of drug (MTX) released from the SLNs cumulatively as a function of time. Figure 4 depicts the in-vitro drug release profile of MTX from pegylated SA-SLNs as well as free MTX at pH 7.4 and 5.5. The drug release was performed at pH 7.4 to simulate the physiological environment and in medium of pH 5.5 to mimic the endosomal/lyosomal microenvironment.[27-30]

Most of the MTX was released into the outside medium at pH 5.5 within the first 3-4h and within 5-6h at pH 7.4. The pegylated SA-SLNs however, exhibited an initial burst effect of almost 30% of the entrapped drug within the first 5h at pH5.5 and about 20% at pH 7.4 around the same time. About 55% of the entrapped drug was released from the SLNs over a period of 48h at neutral pH. But at acidic pH (pH 5.5) almost 73% of the drug was released, indicating a somewhat pH sensitive release of MTX from the SA-SLNs, perhaps owing to the fact that it is closer to the pKa value of MTX. At this rate of release, the drug may get completely released from these SLNs over a period of another 2-4 days and this would be sufficient requirement for this system as tumour delivery does not require sustained release of drug beyond a few days.[3]

Release kinetics: The development of advanced drug delivery systems relies on a judicious and careful selection of components, configurations and geometries, which can be facilitated through mathematical modelling of controlled release systems. The data obtained from in-vitro release studies was modelled to various kinetic equations, viz.-a-viz. the zero order, first order, Higuchi and Korsmeyer-Peppas (Power Law) models, to better understand the underlying mechanism of drug release from the MTX loaded SLNs. Data fitting revealed no correlation with the zero order or first order models (Figure S5(a&b). Nonetheless, the release profiles gave a better fit to the latter two models. Of these, the data showed a closer fit with the Korsmeyer model than the Higuchi model, as also confirmed from the higher r^2 values (regression co-efficient) (Figure S5(c). Further, the plot of drug released as a function of time revealed that the release at acidic pH of 5.5 followed a Fickian release mechanism (n=0.39) while that at pH 7.4 followed an anomalous mode of transport (n=0.517), indicating a superposition of both the Fickian diffusion and the case-II transport.[31] Since different values have been derived for the power law exponent (n) depending on the shape of the carrier system, viz.-a-viz. thin films, cylinders and spheres, we considered the values for

spheres in order to decipher the release mechanism of MTX from the SLNs after confirming the shape of the SLNs from TEM study(Table TS1(a&b)). Thus it was clear from this interpretation that release of MTX from SA-SLNs was solely diffusion controlled at pH 5.5 while at pH 7.4 it was a combination of the dynamic swelling of the carrier system and diffusion controlled release. With these results, it could well be postulated that after systemic administration (pH 7.4), while this SLN formulation is in circulation, the carrier system would be gradually swelling up so as to facilitate complete drug release, whilst the entire formulation would be gradually clearing from the blood stream and moving closer to the target tumour. On reaching the tumour site the drug could start diffusing out easily inside/near the tumour microenvironment due to the existing pH gradient as discussed in details in a later section.

In-vitro cytotoxicity studies

Having studied the drug release kinetics, it was imperative to check whether this carrier system was itself a source of toxicity to the system or not. Therefore, the in vitro cytotoxicity studies of these stearic acid SLNs were carried out by the MTT assay on normal cells (V79 Fibroblast cells). After 12, 24, and 48h of exposure, viability was assessed on the basis of cellular conversion of MTT into a formazan product. A plot of percentage viability versus the concentration showed a decrease in the mitochondrial activity of the drug loaded nanoformulation with increased time of exposure, but not exceeding 60% of the control (Figure 5). These results confirm that these MTX-loaded stearic acid SLNs are nontoxic to normal cells at sub-millimolar concentrations, allowing their use as carriers for chemotherapeutic drugs. These formulations were then taken up for further in-vivo evaluations.

Hemolytic activity

In vitro toxicological assessment of therapeutic nanoparticles has been reported widely, but evaluation of in-vivo toxicity is equally important keeping in mind the usually preferred modes of administration of therapeutic nanoparticles (i.e. oral and intravenous)which involve close contact with blood and its components. For this reason it is pertinent to estimate the degree of interaction of these nanoparticles with human blood components following exposure. Intense to intermediate hemolytic effect has been shown by SLNs based on glycerol monooleate, diglycerol monooleate and glycerol dioleate, especially those stabilized by polysorbate 80. These studies give us reason to believe that these lipid based nanoparticulate formulations need to be used with caution.[32] Therefore hemolytic activity of MTX loaded pegylated SLNs was measured, in order to assess the effects on human RBCs when exposed to these SLNs. Criton X-100(2% aq. Soln.) and PBS pH 7.4(0.15M) were used as positive and negative controls, respectively. Figure 6(A&B) presents the (%) hemolysis induced by various concentrations of these M-P-SLNs upto 4h of incubation as well as a snap shot of the actual suspensions. All the SLN formulations resulted in negligible hemolysis as compared to the positive control (< 1%), and were thus found to be absolutely harmless to RBC membrane integrity, irrespective of the concentration of the drug. This could be attributed to the biocompatible composition of the SLNs as well as the fact that when in contact with blood, the plasma proteins form a protein corona on the particle surface that protects red blood cells from nanoparticles mediated hemolysis.[33]

Radiolabeling studies

Both MTX and MTX loaded pegylated SLNs were labeled with ^{99m}Tc (hereafter referred to as ^{99m}Tc-MTX and ^{99m}Tc-M-P-SLN). All the labeling parameters such as pH, concentration of reducing agents ($SnCl_2$), temperature and incubation time were standardized to achieve the maximum labeling efficiency as reported by our group previously (Figure S6).[34] The proteolytic degradation of the radiolabeled formulations was determined in human serum in vitro. ITLC analysis of the human serum revealed that the ^{99m}Tc-nanoformulations remained sufficiently stable during incubation at 37°C with human serum) (Figure S7). A maximum of 6% of radioactivity degraded after 24h of incubation advocating a high in vitro stability of almost 94% of the nanoformulation for upto 24h. Human serum incubated with $NaTcO_4$ solution (without any nanoforformulation) was taken as control.

In-vivo biological evaluation

A comparative evaluation of the blood clearance studies of the radiolabeled drug and nanoformulation was performed in normal rabbits. Owing to their higher total blood volume (7% of their body weight of 2.5-3.5Kg) than mice, it was easier to withdraw blood (carrying the ^{99m}Tc-labeled compound) at different time points upto 24h, from the same rabbit. The blood clearance profile showed a biphasic mode of clearance from systemic circulation (Figure 7). The radiolabeled drug, ^{99m}Tc-MTX, demonstrated a quicker washout from the blood in a biphasic manner with a fast and slow half-life time of 26.5 mins and 14.2h respectively, and only about 25% of the injected dose remaining after 2h of injection. However, the radiolabeled nanoformulation, ^{99m}Tc-M-P-SLN, exhibited a relatively slower clearance in a somewhat biphasic pattern from the blood circulation, as expected for a pegylated system, with more than 50% of the injected compound remaining in blood 4 h post injection. Nonetheless, about 40 % of the nanoparticulate carriers were eliminated from the blood circulation upto 24h. The rest remained in circulation beyond 24h and was gradually cleared from systemic circulation owing to the small size of the formulations and also perhaps not being readily taken up by the reticuloendothelial system (RES). The $t_{½}$(fast) for the MTX-loaded nanoformulation was found to be 4h, and the $t_{½}$(slow) was 40.2h respectively. At every time point the amount of the labeled M-P-SLN formulation in blood was more than the neat drug, thus suggesting longer blood retention, as also indicated by the half life-time values. This enhanced blood circulation lifetime could easily help facilitate passive targeting of tissues and thus ensure prevalence of the pegylated nanoformulation in the bloodstream for a longer duration of time, than the native drug.

It has been reported that when nanoparticles come in contact with blood, they get coated with a kind of protein-corona, whose quantitative composition defines the bahaviour of the nanocarrier in the circulation as well as the pharmacokinetics and biodistribution of the encapsulated drug.[35] Therefore, protein binding studies were carried out with the above blood samples and they showed a difference in the plasma protein binding of methotrexate (^{99m}Tc-MTX) as compared to its encapsulated form. Binding of ^{99m}Tc-MTX to plasma proteins was found to be around 78% whereas it was 51% in the case of ^{99m}Tc-M-P-SLN nanoformulation probably because of the PEG based matrix.

Figure 8 represents complete tissue distribution after intravenous administration of ^{99m}Tc-MTX and ^{99m}Tc-M-P-SLN and results are expressed as percentage of the injected dose of ^{99m}Tc-labeled compounds accumulated per gram of tissue (%ID/g of tissue) at different time intervals. Appearance of less amount of radioactivity in the stomach at all the time points(less than 2% ID/g) precludes in-vivo decomposition of the radiolabeled nanoformulation to form free $^{99m}TcO_4^-$. Biodistribution study of the drug loaded formulation in tumour bearing mice showed significant localization in tumour muscles due to higher accumulation of MTX in EAT cells, which could be well differentiated as compared to the negligible uptake in the contralateral normal muscles. An increase in survival time is also reported in EAT tumour bearing mice injected(i.p.) with MTX loaded strearic acid SLNs with upto 1.12 fold increase in contrast to MTX conventional injection[23]. The relative tumour uptake of the ^{99m}Tc labeled formulations compared to the contra-lateral normal muscle (tumour:muscle ratio) in balb/c mice is shown in Figure 9, which reveal a significantly high tumour uptake. This was also corroborated by the tumour-to-blood ratios that improved at increasing time points. The whole body SPECT imaging in rabbits (Figure 10) clearly showed renal clearance of ^{99m}Tc-MTX at 4h p.i. while the radiolabeled nanoformulation showed uptake in tissues with leaky endothelial walls viz.-a-viz. liver, spleen and tumours as reported for nanoparticles.[36,37] The radiolabeled formulation showed uptake to a higher level in the liver and kidneys at early time points after injection. However, with the passage of time as the protein binding (primarily opsonisation) of the particles gets minimized, this preferential uptake by macrophages and tissues also gets reduced, as is seen in a later whole body image at 22h time point. The route of excretion of the nanoformulation was therefore perceived to be both renal and hepatobiliary. This clearly indicated that these nanoparticulate carriers eventually get eliminated from the body. Nonetheless, the important aspect that the intracellular tumour uptake of the particles is not compromised was verified by SPECT imaging of tumour mice injected with radiolabeld MTX and M-P-SLN. The MTX loaded formulation showed much higher uptake in tumour muscles as compared to that of ^{99m}Tc-MTX at a 4h time point (Figure 11). This tumour uptake could be expected to increase further with the passage of time as the RES uptake gradually reduced and the blood to tumour uptake of the nanoformulation increased. This uptake helped to clearly delineate the tumour from the rest of the normal muscle, corroborated by the whole body tumour scintigraphic image.

DISCUSSION

Nanocarriers have been widely reported to be taken up by cells through endocytosis and to a lesser extent by the diffusion through the cell membrane.[38] During their transport to the tumour cells the nanoparticles encounter a gradual change in pH from 7.4 in blood stream to 7.01 in the tumour extracellular fluid. On entering the tumour cells via endocytosis the pH drops to as low as 5-6 in the endosomes and 4-5 in the lysosomes. These differences in pH between the normal tissues and the tumour tissues as well as the acidic environment in endosomal and lysosomal compartments can well act as an internal stimulus to trigger drug release inside the cell on particle disruption.[39] This could be explained by the current study where the MTX entrapped in the pSLNs is found to release faster at an acidic pH under in-vitro conditions. The current study also reveals a low residence time of MTX inside the tumour cells, as shown by the decreased uptake in tumour tissue at longer time points beyond 4h, in the biodistribution studies. This could be explained by the fact that the native drug is reported to be effluxed out of the cells with the help of lysosomes, resulting in MDR in tumour cells[40], which however seems to be decreased or absent in case of the pSLNs. Therefore, in our opinion the receptor mediated influx of MTX-loaded pSLNs and the reduced efflux could well explain their enhanced tumour uptake and residence time at the tumour site, as also explained by the biodistribution studies and further supported by the scintigraphic analysis.

At the same time slow release at physiological pH of 7.4, accompanied by enhanced blood circulation of pegylated SLNs will give added advantage as it gives sufficient time for gradual uptake by the target tissues and organs, especially the tumour cells which have overexpressed folate receptors. Therefore, this MTX-loaded pegylated SLN formulation has the potential to decrease the frequency of injection so as to maintain the therapeutic dosage of MTX for a desired interval.

Experimental

Materials and Methods

Materials

Polyethylene glycol (MW 4000), Methotrexate (MTX) and Tween-80 were procured from M/s Sigma Aldrich, USA. Stearic Acid (SA), soyalecithin and Criton X-100 were procured from CDH fine chemicals, Delhi, India. Technetium-99m was procured from Regional center for radiopharmaceuticals (Northern region), Board of Radiation and Isotope Technology (BRIT), Department of Atomic Energy (DAE), INMAS Centre, Delhi. For PEG-Stearate characterization, Infrared spectra (FTIR) were recorded by the KBr pellet method in the range of 4000 – 400 cm^{-1} on a Perkin Elmer Spectrum BX-II spectrophotometer (Perkin Elmer, Beaconsfield, UK) and ^{1}H NMR were recorded on a Bruker Avance II 400MHz system

(Bruker Corporation, Fallanden, Switzerland) in D_2O solvent. UV-Vis scanning was done on a single beam UV-Vis spectrophotometer, (Spectra Max M2, Molecular Devices), as per reported literature.[41] Gamma ray spectrometer (type GRS23C)(Electronics Cooperation of India Pvt. Ltd., India, was used for determining the amount of activity (γ-emitter) in the samples. Gamma scintillation camera installed at INMAS(HAWKEYE) was used for SPECT imaging of animals.

Tumour models for in-vivo evaluation

Balb/c mice of either sex (six to eight weeks old, weighing 25-30 g) with no prior drug treatment were used for biodistribution studies and gamma imaging. Tumour models were prepared by inoculating the mice with ~$15x10^6$ Ehrlich Ascites Tumour (EAT) cells. Healthy, New Zealand Albino rabbits (2.5-3 Kg) were employed for blood kinetics studies. Animals were housed at the in-house facility under conditions of controlled temperature (22±2°C) and fed on normal diet. All animal experiments and study protocols were approved by the institutional ethical committee of INMAS, Government of India, Delhi.

Preparation and purification of MTX loaded SLN formulations

MTX-loaded SLNs were prepared by the solvent diffusion method in aqueous system.[42,43] Initially a 1:1 mixture of ethanol-acetone was mutually saturated with water at 47±2°C for 10 min to ensure thermodynamic equilibrium of both liquids. Specified amount of lipid, stearic acid, was then dissolved in this organic phase in a water bath at 50°C, to obtain a series of formulations in which the lipid and the surfactant concentration were varied in order to evaluate their influence on particle size (Table TS1(a)). A specified ratio of the drug, varied between 0.1-1.0, was set to the lipid quantity, and dispersed in 50mL of the aqueous phase which was a 1.5% solution of a surfactant and co-surfactant combination (Tween-80 and Soya-Lecithin (1:1)) in 50ml distilled water. This was found to be the optimized concentration and ratio of the surfactant and co-surfactant combination after performing studies on 0.5:1, 1:1, 1.5:1, 1:0.5, 1:1.5 ratios and 0.5-2% variation in concentration of each ratio).[44] Higher concentrations of surfactant solution resulted in precipitation. A combination of surfactant and co-surfactant was used for the formulations as SLNs stabilized with a mixture of surfactants have shown smaller particle sizes and higher storage stabilities.[45] The pH of the aqueous phase was adjusted to 1.10 with HCl in order to avoid coacervation of the SLNs. The lipid solution was then emulsified with this acidic aqueous phase under continuous mechanical agitation at 4000 rpm at room temperature (22-24°C) for 5 min). The resulting SLN dispersion was sonicated in a bath sonicator for 10 min followed by sonication in a probe sonicator for 40 cycles with 10sec on and 5 sec off each. (VCX 750 Vibracell™, Sonics & Materials, Inc., Newton, CT, USA using the 13mm probe with amplitude 30%). The unloaded control SLNs were prepared similarly without the addition of drug. For the pegylated SLNs, PEG-monostearate synthesized previously (supplementary information) was added as per Table TS1(b). The rest of the procedure was the same as described above.

The SLN dispersions were purified by utrafiltration with an ultrafiltration unit (Merck Millipore, Darmstadt, Germany) using a 10,000Da cut-off membrane. The first 50 ml of suspension were concentrated to 10 ml, then 10 ml additional water was added and the suspension reconcentrated to 10 ml. This procedure was repeated a further three times to obtain the purified SLN dispersion in aqueous medium, devoid of any organic solvent and acidic phase. The pH of the SLN dispersion after purification was checked to be neutral (~7.0). The prepared dispersions were lyophilized to prepare samples for DSC analysis (Freezone 2.5plus, Labconco Corporation, MO, USA).

SLN Characterization

Particle Size and zeta potential analysis: The average hydrodynamic diameter, polydispersity index(PDI) and Zeta potential of the ultrafiltrated formulations were determined by the laser light scattering technique (Malvern Zetasizer 90S, UK). Measurements were made in triplicate for all the batches prepared.

Transmission electron microscopy (TEM) and AFM: The morphology of the MTX loaded pegylated and non-pegylated SLNs were characterized by TEM(HITACHI, H-7500, Japan). Samples were prepared by spraying the aqueous formulation on a copper grid (200 mesh size, carbon coated). AFM images were recorded with an AFM microscope in the tapping mode (ScanAsyst®, Bruker, USA). A drop of the SLN formulation was placed on a clean mica surface, air dried and then observed by AFM.

Thermal characterization by DSC: DSC analysis was performed on a TA Instruments differential calorimeter with a liquid nitrogen cooling accessory (Model No. Q10, TA instruments, Waters Inc., USA). Hermetic pans having ~4mg dry sample were heated from 50–300°C at a rate of 10°C /min in nitrogen atmosphere and subsequently cooled at the same rate. Thermograms were then recorded at a heating rate of 10°C /min over a temperature range of 50–300°C. All the samples were subjected to the same thermal cycles.

In vitro release and kinetics study

Drug release from the pegylated and non-pegylated SLNs was monitored by the dialysis method. Aqueous suspensions of the drug loaded SLNs were analyzed spectrophotometrically at 303nm, in order to quantitatively estimate the MTX released. For comparison, MTX released from the stock solution was also conducted under the same conditions. The measurements were repeated three times using different samples from independent preparations. The entrapment efficiency (% EE) and drug loading (%DL) of MTX in the SLNs was determined by disrupting the drug loaded SLNs in 1ml of DMSO. The drug content in DMSO was determined by UV-spectrometry at 303nm. The %EE and %DL were were calculated as follows:

$$Drug\ Loading\ Efficiency(\% = (Mass\ of\ MTX\ encapsulated\ in\ SLNs) / (Mass\ of\ MTX\ added) x\ 100$$

$$Drug\ Loading\ Capacity(\%) = (Mass\ of\ MTX\ in\ SLNs) / (Mass\ of\ SLNs) x 100$$

The in vitro release profile was studied in acetate buffer (pH 5.5) and 0.1M PBS buffer (pH 7.4) using a Spectra-Por® Float-a-lyzer (MWCO 8kDa, Spectrum Laboratories, USA). The Float-a-lyzer was soaked in distilled water for 12h before mounting in the dialysis set-up. 10 ml of the SLN formulations (pegylated and non-pegylated) were placed in the Float-a-lyzer and the receptor compartment was filled with 100ml of dialysis medium (buffer pH 5.5 or pH 7.4). 2ml of sample was withdrawn from the receiver compartment to determine the absorbance by UV. An equal quantity of fresh medium was added to maintain sink conditions. Calibration curves of MTX in acetate buffer and PBS (given in supplementary information) were used to calculate the drug concentration in the SLNs (Figure S1). The control SLNs without MTX were treated similarly and used as blank for the measurements. The cumulative percentage drug release was calculated using the equation:

$$\%\ Drug\ Release = \left[1 - \left\{\frac{Absorbance(t)}{Absorbance(t0)}\right\}\right] x\ 100$$

't' being the time at which the absorbance is measured and 't0' the initial time.

To investigate the mechanism of drug release from the MTX loaded SLNs, the release data was plotted as per various kinetic models viz.-a-viz. zero order, first order, Higuchi square root and Korsmeyer-Peppas models to analyze the in vitro release. The mathematical expressions that describe the models used to evaluate the dissolution curves are tabulated in Table TS1 (a&b).

Cytotoxicity of nanoformulations

Cytotoxicity of the SLNs and MTX loaded SLNs was determined using V79 fibroblast cells, by the MTT {3-4,4-dimethylthiazole-2-yl)-2,5-diphenyl-2H-tetrazolium bromide} assay. Cells were treated with bare SLNs and MTX-loaded SLNs (containing 5mM drug) and incubated for different time intervals; 12, 24 and 48h. Untreated cells acted as positive control and cells treated with 1%(v/V) Triton X100 as negative control. At the end of the treatment the cells were incubated with MTT at a final concentration of 0.5 mg/ml for 2h at 37°C and the medium was removed. The cells were lysed and the formazan crystals were dissolved using 150µl of DMSO. Optical density was measured on 150µl extracts at 570nm (reference filter: 630nm). Mitochondrial activity was expressed as percentage of viability compared to negative control. Percentage viability = $[OD(570nm\text{-}630nm)_{test\ product}/OD(570nm\text{-}630nm)_{negative\ control}]$ x 100.

Hemolytic activity

Hemolytic activity of the native drug (MTX) and the MTX-loaded pegylated SLNs was evaluated by a previously reported method.[46] Briefly, blood was drawn from healthy human volunteers, with prior consent, and placed into citrated vaccutainers (BD, NJ, USA). This was centrifuged at 3000rpm for 10 mins in order to separate the RBCs from the plasma. The RBC pellet obtained was washed thrice with saline and the washed pellet was suspended in 48 ml of PBS (pH 7.4) to prepare a RBC suspension. In each case, 200µL of sample (MTX solution and MTX loaded SLN dispersion with equivalent MTX concentration) was mixed with 800 µL of the RBC suspension. These were incubated after gentle mixing at 37˚C for different time points from 15min-4h to evaluate the time dependent hemolytic character of the compound. Thereafter, 2ml of the mixture was centrifuged for 10min at 3000 rpm for erythrocytes to precipitate. The supernatant's optical density at 540nm was measured by UV-Vis spectrophotometer and the (%) hemolysis was calculated using the following formula:

$$\%\text{Hemolysis} = \frac{(Absorbance_{compound} - Absorbance_{-ve\ control})}{(Absorbance_{+ve\ control} - Absorbance_{-ve\ control})} \text{ x } 100$$

Radiolabeling of nanoformulations

Both the drug loaded and unloaded formulations were labeled with ^{99m}Tc by the direct labeling method. Briefly, 100 µL of a freshly eluted sterile solution of sodium pertechnetate in saline (containing approx. 74-110 MBq of $^{99m}TcO_4^-$ obtained by solvent extraction method from Molybdenum) was added to 100 µL (1 mg/mL) of each formulation followed by addition of 150 µL stannous chloride solution (2 mg/mL in N_2 purged 10% glacial acetic acid); pH was adjusted to 7.0 using 0.1 M NaOH/0.1 M acetic acid, and the resulting solution was incubated at 37˚C for 20 mins. The labeled formulations, thus obtained, were stored in sterile shielded vials for subsequent studies. The radiochemical purity and radiolabeling efficiency of formulations was determined by ascending instant thin layer chromatography (ITLC) as reported in literature.[47]

In vitro human serum stability

The metabolic stability of the nanoformulations was ascertained in vitro in freshly collected human serum from healthy volunteers. 100 µL of ^{99m}Tc labeled formulations were incubated respectively in 900 µL of this serum (in duplicate) at 37°C and analyzed to check for any dissociation of the complex by ITLC using silica gel strips and 0.9 % NaCl aqueous solution (saline) as developing solvent. The change in labeling efficiency was monitored over a period of 24 h.

In vivo evaluation

Blood Clearance and Plasma Protein binding studies in rabbits: Blood clearance of ^{99m}Tc-labeled SLNs and ^{99m}Tc-labeled MTX was studied in healthy New Zealand Albino rabbits weighing 2.5-3.5 kg (n=3). 300 µL of the individual radiolabeled complexes (10 MBq) were administered intravenously through the dorsal ear vein. Blood samples were withdrawn from the other ear vein at different time intervals ranging from 5 mins-24 h. Persistence of activity in the circulation was calculated as percentage injected dose per whole blood, assuming total blood volume as 7% of the body weight. The radioactivity of the

precipitate and supernatant was measured in a well-type gamma spectrometer.

Using the above blood samples, plasma was separated out by centrifugation, and the plasma proteins were precipitated by addition of 10% trichloroacetic acid (TCA). The radioactivity of the precipitate and supernatant was measured in a well-type gamma spectrometer.

Biodistribution in Mice: Ascitis tumour bearing mice were administered 100 µL (3.7 MBq) of ^{99m}Tc labeled formulations, respectively, through the tail vein (i.v.). At 1, 2, 4 and 24 h post injection, the animals (n=3) were euthanized and blood was collected by cardiac puncture into pre-weighed tubes. The mice were then dissected and various organs (heart, lungs, liver, spleen, kidneys, stomach, intestine, bone, muscle (normal and tumour) and brain) were removed, weighed and their radioactive uptake was measured with the help of a gamma counter. Uptake of the radiolabeled compound into each organ was measured per gram of the tissue/organ and expressed as percentage injected dose per gram organ weight. The radioactivity remaining in the tail (point of injection) was also measured and taken into account while calculating the radioactivity.

Gamma Scintigraphy in murine tumour models: The tumour bearing mice were administered 100 µL (3.7MBq) of ^{99m}Tc labeled formulations, respectively(i.v.), through the tail vein and gamma imaging was performed at different time intervals using a planar gamma camera equipped with a collimator, in order to visualize the in-vivo uptake of the ^{99m}Tc-labeled nanoformulations.

Conclusions

This research work profiles the preparation of stearic acid based pegylated SLNs(<150 nm in size) and their ability to effectively entrap the chemotherapeutic drug MTX at low pH, which normally presents very low bioavailability in the body. The minimal cytotoxicity and negligible RBC toxicity proves these pegylated SLNs to be a safe drug carrier, however further optimization may prove helpful in this respect. The pharmacokinetic studies in rabbits along with the high tumour uptake in animal models validate the potential of these pegylated SLNs as a useful therapeutic approach to enhance the bioavailability of MTX by pegylating its carrier system. All the investigations carried out as part of this work gave adequate evidence that these pegylated SLN formulations may have potential applications as nanoparticulate carriers of chemotherapeutic cargos like methotrexate, to aid in enhanced antitumour efficacy and reduced systemic toxicity of such onco-medicines. However, detailed studies on tumour proliferation rate in animal models can give significant inputs on the therapeutic efficacy of these developed pegylated SLNs, which can form part of our future studies.

Acknowledgements
This work has been carried out under Project INM-311(3.1). We thank Dr. R. P. Tripathi, Director INMAS, for providing necessary facilities and infrastructure for carrying out this research work. Financial assistance provided to SD by CSIR, India, is duly acknowledged.

Notes and references

Division of Cyclotron and Radiopharmaceutical Sciences, Institute of Nuclear Medicine and Allied Sciences, Brig. S.K. Mazumdar Road, Timarpur, Delhi-110054, India. Fax:+911123919509, E-mail: diptikakkar@gmail.com, akmisra@inmas.drdo.in

† **Electronic Supplementary Information (ESI) available: Table TS1** gives gives the mathematical equations of models used to describe drug release . **Figures S1 to S7** give the calibration curves of MTX in acetate buffer and PBS, FTIR and NMR spectra of the synthesized PEG-Stearate, FTIR spectra of the MTX loaded pegylated formulation, in vitro release profile of free MTX, Optimization of radiolabeling parameters and in vitro serum stability of ^{99m}Tc labeled MTX and M-P-SLN. See DOI: 10.1039/b000000x/

1 I. Brigger, C. Dubernet and P. Couvreur, *Adv. Drug Deliv. Rev.*, 2012, **64**, 24-36.
2 P. Severino, T. Andreani, A. Jager, V.C. Marco, H.A.S. Maria, M.S. Amelia and E.B. Souto, *Eur. J. Med. Chem.*, 2014, **81**, 28-34.
3 J. V. Natarajan, C. Nugraha, X. W. Ng and S. Venkatraman, *J. Control. Release*, 2014, **193**, 122.
4 A. J. Almeida and E. Souto, *Adv. Drug Deliv. Rev.*, 2007, **59**, 478-490.
5 A. Pozo-Rodríguez, D. Delgado, M. Á. Solinís, J. L. Pedraz, E. Echevarría, J. M. Rodríguez and A. R. Gascón, *Int. J. Pharm.*, 2010, **385**, 157-162.
6 D. K. Thukral, S. Dumoga and A. K. Mishra, *Curr. Drug Deliv.*, 2014, **11**, 771-791.
7 E. Rostami, S. Kashanian, A. H. Azandaryani, H. Faramarzi, J. E. Dolatabadi and K. Omidfar, *Chem. Phys. Lipids.*, 2014, **181**, 56-61.
8 J. Zheng, Y. Wan, A. Elhissi, Z. Zhang and X. Sun, *Pharm. Res.*, 2014, **31**, 2220-2233.
9 J. Varshosaz, P. M. Ghalaei and F. Hassanzadeh, *J. Nanomat.*, 2014, DOI: 10.1155/2014/345845.
10 J. Madan, R. S. Pandey, V. Jain, O. P. Katare, R. Chandra and A. Katyal, *Nanomedicine*, 2013, **9**, 492-503.
11 A. Chonn and P.R. Cullis, *J. Liposome Res.*, 1992, **2**, 397-410.
12 M. D. Howard, X. Lu, J. J. Rinehart, M. Jay and T. D. Dziubla, *Langmuir*, 2012, **28**, 12030-12037.
13 H. Yuan, C. Y. Chen, G. H. Chai, Y. Z. Du and F. Q. Hu, *Mol. Pharm.*, 2013, **10**, 1865-1873.
14 A. B. Jaber, H.Cui, A. Elsaid, M. Yalcin, T.Sudha and S.A. Mousa, *ScienceJet*, 2015, **4**, 145.
15 S. Kashanian and E. Rostami, *Journal of Nanoparticle Research*, 2014, **16**, 2293.
16 K. Knop, R. Hoogenboom, D. Fischer and U. S. Schubert, *Angew Chem. Int. Ed. Engl.*, 2010, **49**, 6288-6308.

17 S. Yoon, J. R. Choi, J. O. Kim, J. Y. Shin, X. Zhang and J. H. Kang, *Cancer Res. Treat.*, 2010, **42**, 163-171.
18 M. M. Mader, J. R. Henry, in Antimetabolites, ed. J. B. Taylor, D. J. Triggle, Elsevier Ltd., Oxford, UK, 2007, pp. 55-79.
19 N. A. Kasim, M. Whitehouse, C. Ramachandran, M. Bermejo, H. Lennernäs, A. S. Hussain, H. E. Junginger, S. A. Stavchansky, K. K. Midha and V. P. Shah, *Mol. Pharm.*, 2004, **1**, 85-96.
20 Z. A. Khan, R. Tripathi and B. Mishra, *Expert Opin. Drug Deliv.*, 2012, **9**, 151-169.
21 J. Chen, L. Huang, H. Lai, C. Lu, M. Fang, Q. Zhang and X. Luo, *Mol. Pharm.*, 2014, **11**, 2213-2233.
22 A. Misra, M. Kalariya, B. K. Padhi and M. Chougule, *Drug Deliv. Technol.*, 2002, **5**, 1-13.
23 K. Ruckmani, M. Sivakumar and P. A. Ganeshkumar, *J. Nanosci. Nanotechnol.*, 2006, **6**, 2991-2995.
24 B. Bhagya, R. Parthibarajan, S. Pradeep Kumar and C. Srinivas, *Der. Pharmacia Lettre*, 2014, **6(4)**, 335-342.
25 K. Thode, R. H. Muller and M. Krese, *J. Pharm. Sci.*, 2008, **89**, 1317-1324.
26 H. Bunjes, B. Siekmann and K. Westesen, in Emulsions of supercooled melts – a novel drug delivery system, ed S. Harwood Academic Publishers, Amsterdam, Netherlands, 1998, pp. 175-204.
27 K.N. Yang, C.Q. Zhang, W. Wang, P. C. Wang, J. P. Zhou, and X. J. Liang, *Cancer Biol Med.*, 2014, **11(1)**, 34–43.
28 S. C. Wuang, K. G. Neoh, E. T. Kang, D. E. Leckband, and D. W. Pack, *AIChE J*., 2011, **57(6)**, 1638–1645.
29 Q. Miao, D. Xu, Z. Wang, L. Xub, T. Wang, Y. Wua, D. B. Lovejoy, D. S. Kalinowski, D. R. Richardson, G. Nie and Y. Zhao, *Biomaterials*, 2010, **31**, 7364-7375.
30 L. Xie, W. Tong, D. Yu, J. Xu, J. Lib and C. Gao, *J. Mater. Chem.***,** 2012,**22**, 6053-6060.
31 J. Siepmann and N. A. Peppas, *Adv. Drug Deliv. Rev.*, 2001, **48**, 139-157.
32 T. Mocan, *Biotechnology, Molecular biology and Nanomedicine*, 2013, **1**, 7-12.
33 K. Saha, D. F. Moyanoa and V. M. Rotello, *Mater. Horiz.*, 2014, **1**, 102-105.
34 D. Kakkar, A. K. Tiwari, K. Chuttani, A. Kaul, H. Singh and A. K. Mishra, *Cancer Biother. Radiopharm.*, 2010, **25**, 645-655.
35 N. R. Kuznetsova and E. L. Vodovozova, *Biochemistry Moscow*, 2014, **79**, 797-804.
36 D. E. Owens and N. A. Peppas, *Int. J. Pharm.*, 2006, **307**, 93-102.
37 S. D. Li and L. Huang, *Mol. Pharm.*, 2008, **5**, 496-504.
38 S. Dawar, N. Singh, R. K. Kanwar, R. L. Kennedy, R. N. Veedu, S. Zhou, S. Krishnakumar, S. Hazara, S. Sasidharan, W. Duan and J. R. Kanwar, *Drug Discov. Today*, 2013, **18**, 1292-1300.
39 Y. Liu, W. Wang, J. Yang, C. Zhou and J. Sun, Asian *J. Pharm. Sci.*, 2013, **8**, 159-167.
40 Y. G. Assaraf, *Drug Resistance Updates*, 2006, **9**, 227-246.
41 D. Kakkar, A.K. Tiwari, K. Chuttani, R. Kumar, K. Mishra, H. Singh and A.K. Mishra, *Ther. Deliv.*, 2011, **2**, 205-212.
42 F. Q. Hu, H. Yuan, H. H. Zhang and M. Fang, *Int. J. Pharm.*, 2011, **239**,121-128.
43 H. Yuan, L. F. Huang, Y. Z. Du, X. Y. Ying, J. You, F. Q. Hu and Su. Zeng, *Colloids Surf. B Biointerfaces*, 2008, **61**, 132-137.
44 M. A. Schubert and C. C. Müller-Goymann, *Eur. J. Pharm.*, 2005, **61**, 77-86.
45 H. Bunjes, M. H. Koch and K. Westesen, *J. Pharm. Sci.*, 2003, **92**, 1509-1520.
46 G. P. A. K. Michannetzis, Y. F. Missirlis and S. G. Antimisiaris, *J. Biomed. Nanotechnol.*, 2008, **4**, 218.
47 D. Kakkar, A. K. Tiwari, K. Chuttani, A. Khanna, A. Datta, H. Singh and A. K. Mishra, *Chem. Biol. Drug Des.*, 2012, **80**, 245-253.

TABLES

Table 1: Composition of Pegylated and non-Pegylated SLNs

Formulation	Lipid Stearic acid (mg)	PEG (wt %)	Surfactant:Cosufactant Tween80: Soyalecithin (wt %)	Size (nm)	PDI	Zeta Potential (mV)
SA1	55	-	0.5%	135.8±2.59	0.28±0.03	-
SA2	110	-	0.5%	204.6±1.84	0.47±0.01	-
SA3	55	-	1.0%	137.4±0.23	0.21±0.02	-
SA4	110	-	1.0%	219.9±0.84	0.12±0.02	-
SA5	**55**	**-**	**1.5%**	**156.7±0.76**	**0.13±0.01**	**-**
SA6	110	-	1.5%	214.2±1.48	0.38±0.03	-
SD1	55	10	1.5%	154.4±22.8	0.137±0.01	-56.4±8.7
SD2	55	20	1.5%	142.8±11.6	0.229±0.02	-43.8±7.5
SD3	55	40	1.5%	139.2±3.2	0.218±0.02	-39.2±1.3
SD4	**55**	**80**	**1.5%**	**127.5±1.7**	**0.152±0.01**	**-34.7±0.9**

Table 2: Drug Loading and encapsulation efficiency of Pegylated SLNs

Formulation	Drug:Lipid (wt %)	Particle Size (nm)	Zeta Potential	Polydispersity Index (PDI)	Encapsulation Efficiency (%)	Drug Loading (%)
PSD 1	0.1 : 1	113.2±4.9	-14.28±1.6	0.52±0.02	51.84	9.92
PSD 2	0. 2: 1	129.7±8.2	-16.33±2.13	0.14±0.01	62.91	6.32
PSD 3	0.4: 1	128.8±0.36	-22.7±5.99	0.261±0.01	65.38	15.16
PSD 4	**0.6: 1**	**129.7±0.86**	**-34.0±6.37**	**0.211±0.01**	**70.22**	**22.31**
PSD 5	0.8 : 1	137.8±1.65	-30.5±1.8	0.38±0.02	70.38	28.25
PSD 6	1 : 1	138.6±2.1	-27.2±2.6	0.42±0.02	71.46	20.22

Table 3: Biodistribution profile of ^{99m}Tc-labeled free MTX in tumour mice

ORGAN/Time	1 h	2 h	4 h	24 h
Blood	1.62	1.24	0.78	0.16
Heart	0.56	0.40	0.305	0.10
Lungs	1.235	0.96	0.79	0.39
Liver	14.55	10.06	8.28	4.335
Spleen	3.46	2.71	2.13	1.16
Kidneys	1.79	1.30	0.91	0.535
Stomach	0.56	0.40	0.265	0.14
Intestines	0.32	0.27	0.195	0.07
Brain	1.185	1.50	1.215	0.53
Bone	0.03	0.04	0.04	0.01
Muscle	0.83	0.27	0.146	0.08
Tumour	1.495	1.04	0.89	0.155

Values are %ID/gm tissue weight

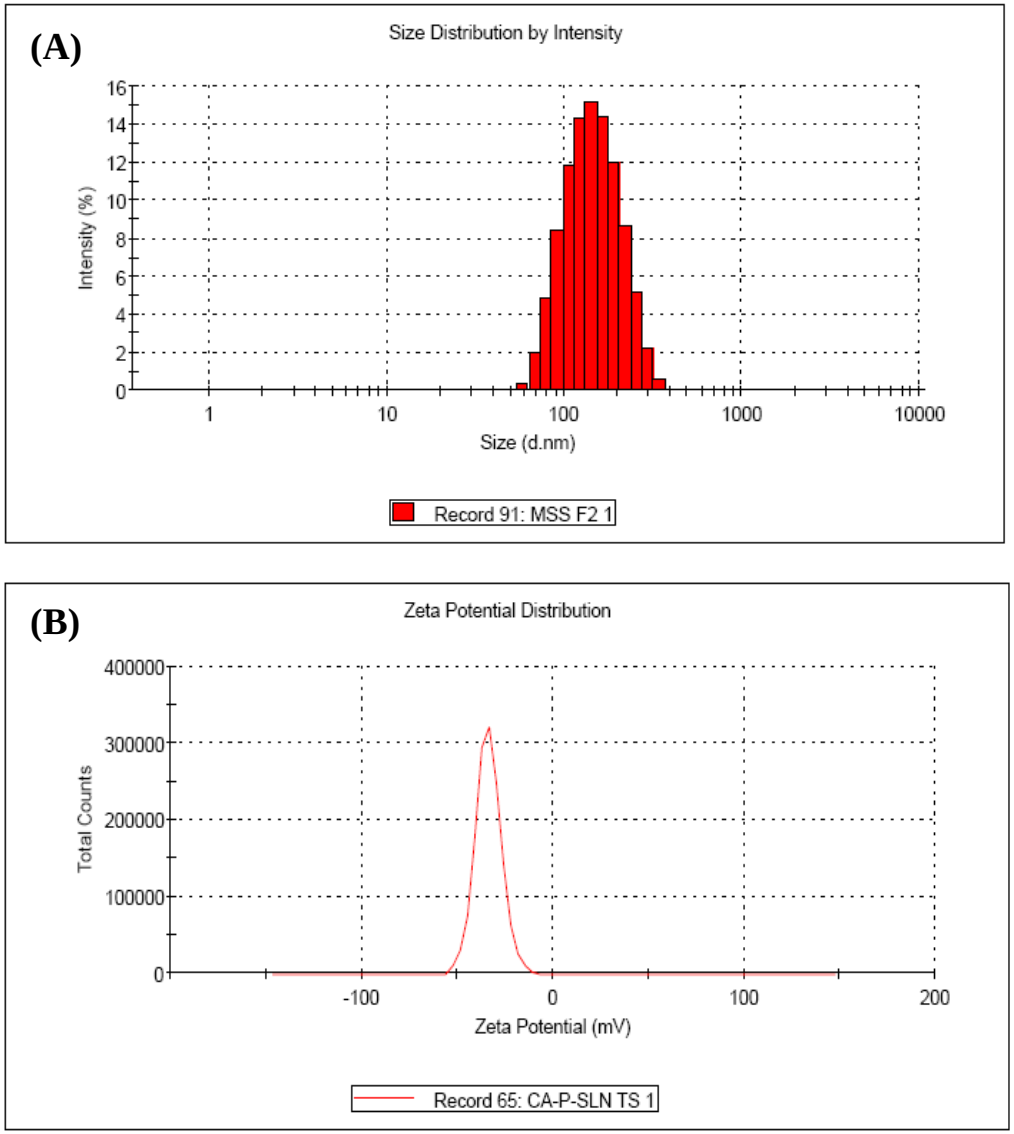

Fig 1: (A) Size and (B) Zeta Potential measurements of M-P-SLNs formulation

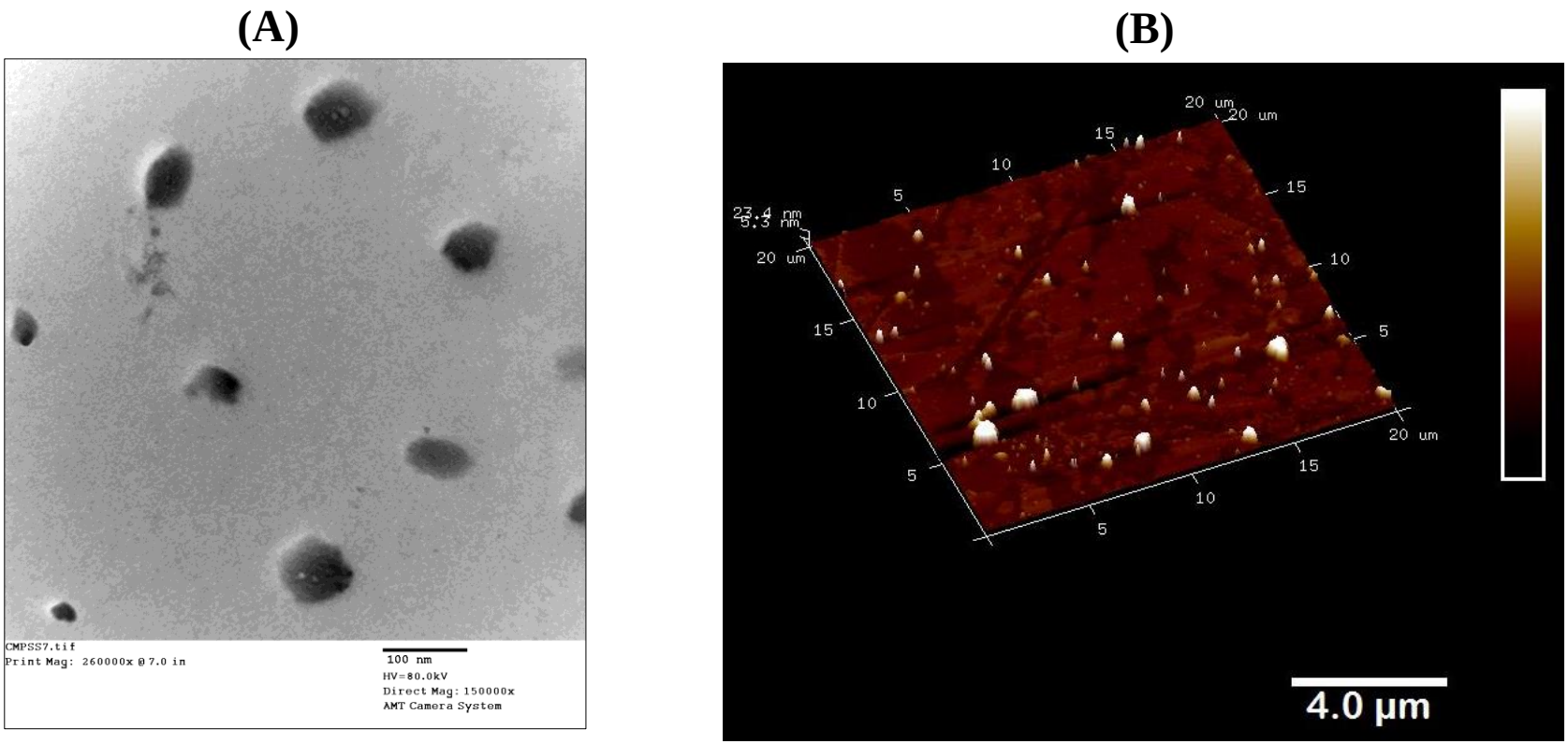

Fig 2: (A)TEM and (B)AFM images of M-P-SLNs

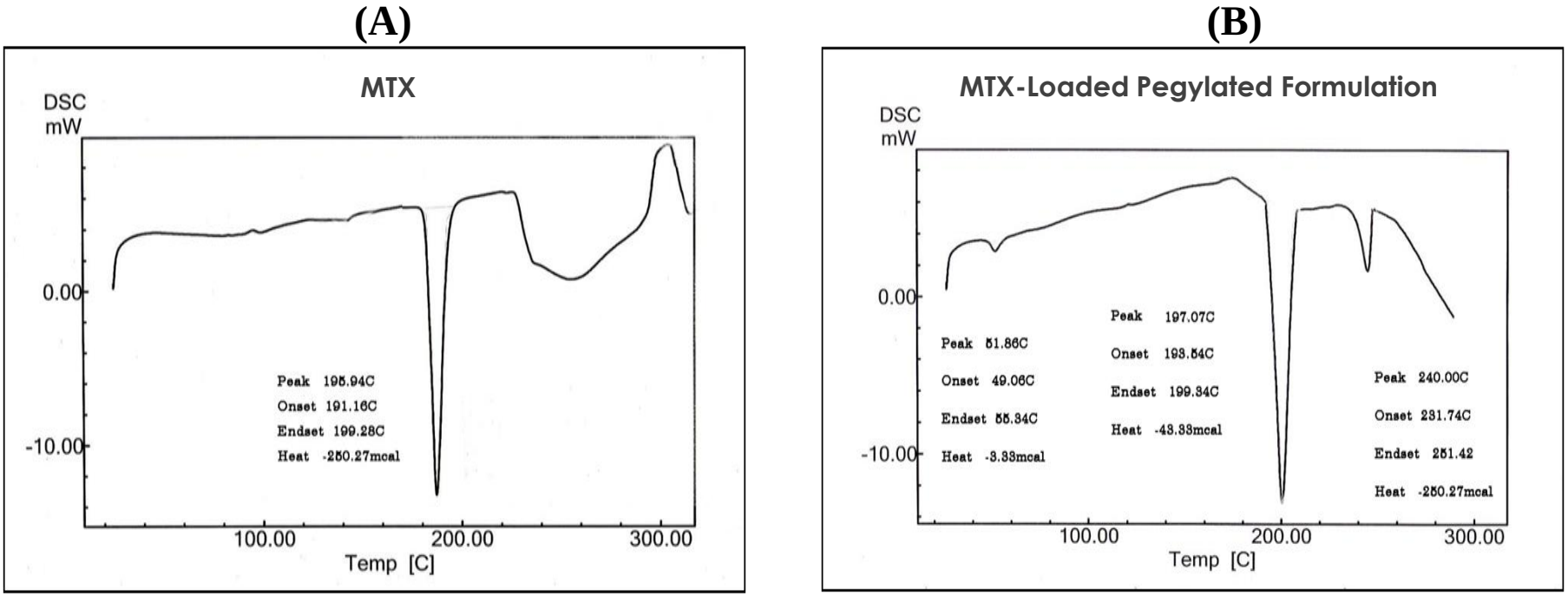

Fig 3: DSC curves of (A)MTX and (B)M-P-SLNs

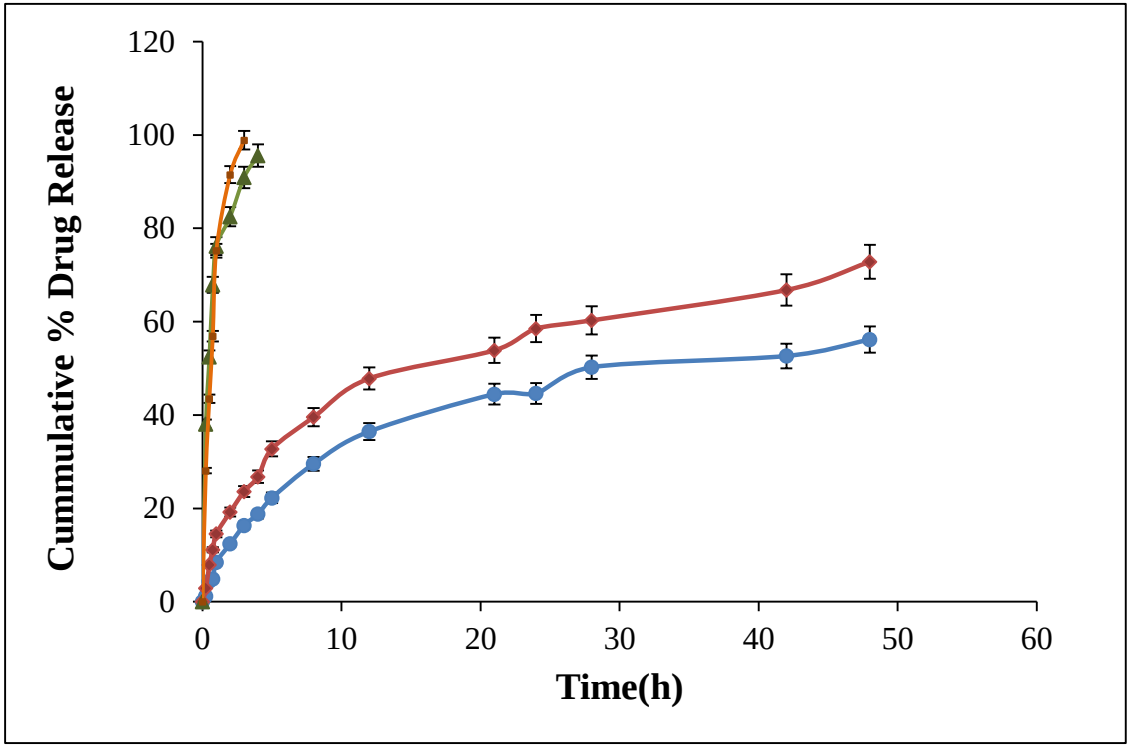

Fig 4: In vitro Drug release profile of free MTX and M-P-SLN formulation over 48h at pH 5.5 and 7.4. Each point represents the mean value ± SD(n=3)

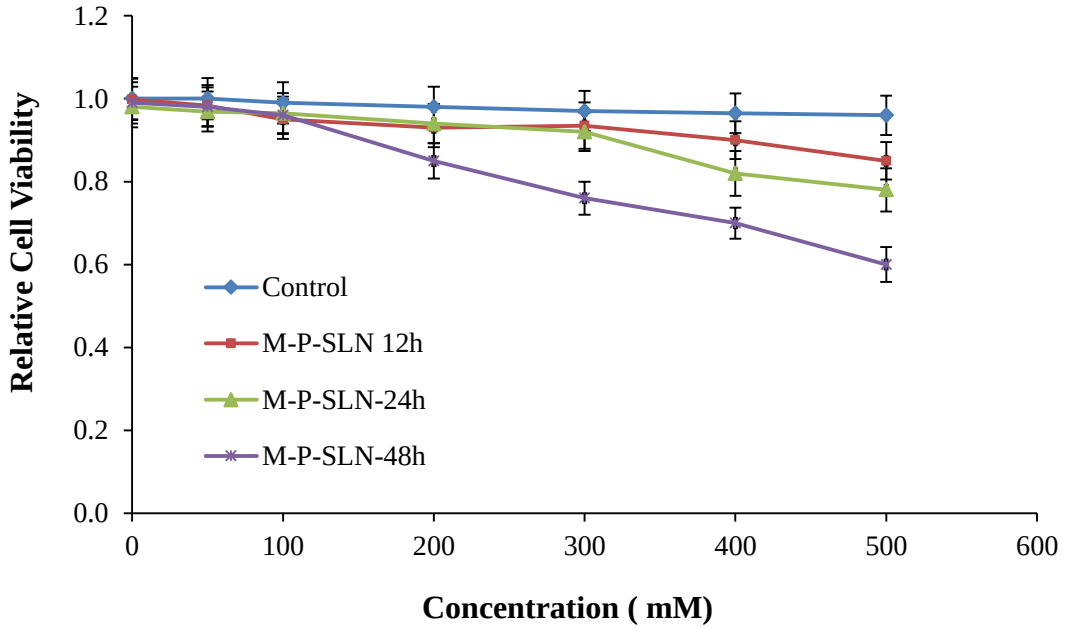

Fig 5: In vitro cytotoxicity of M-P-SLNs after 12, 24 and 48h of incubation

Control Mp-SLN 12h Mp-SLN-24h Mp-SLN-48h

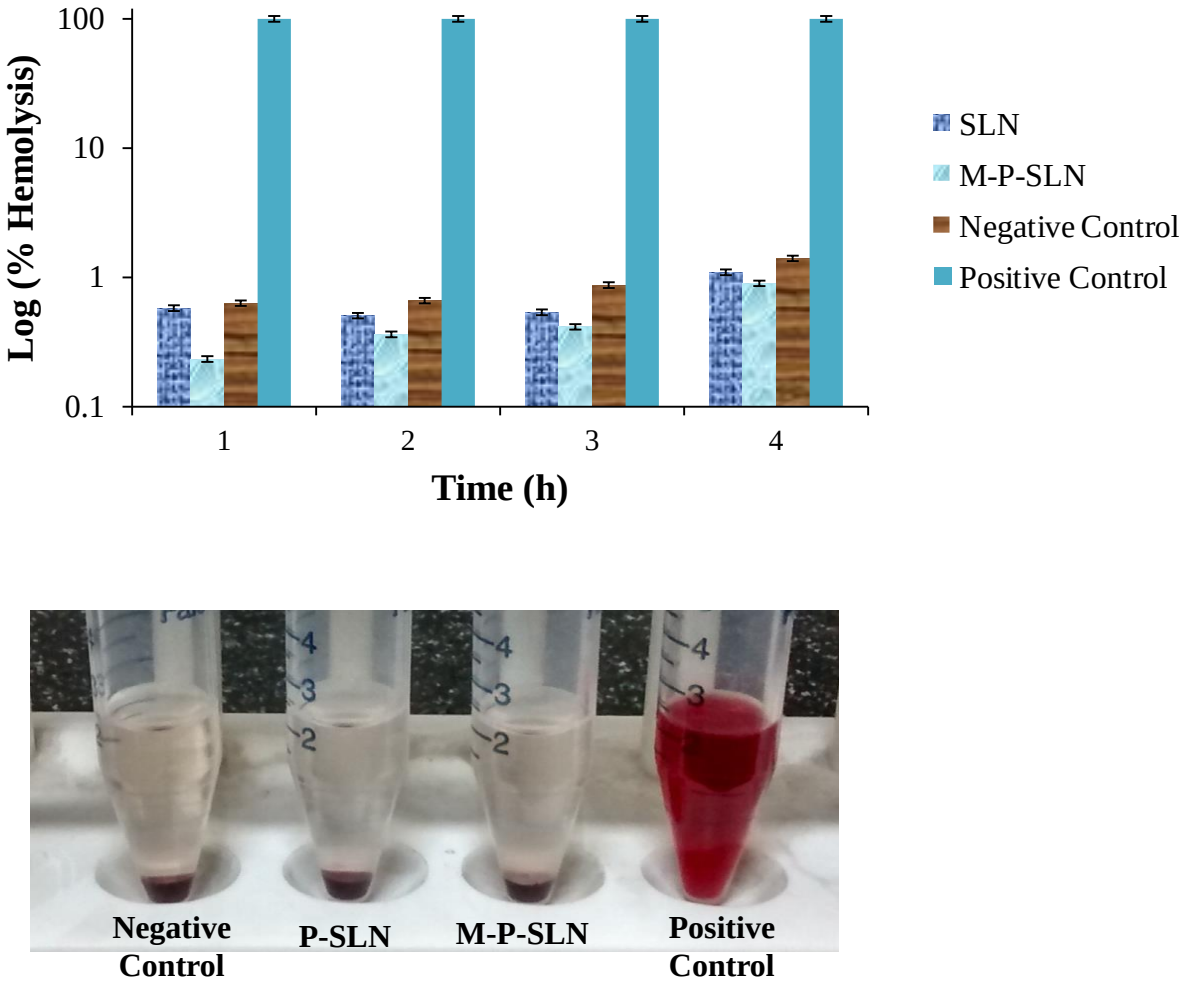

Fig 6: (A) Hemolytic activity of M-P-SLNs after 4h of incubation; (B) Actual samples showing hemocompatibility

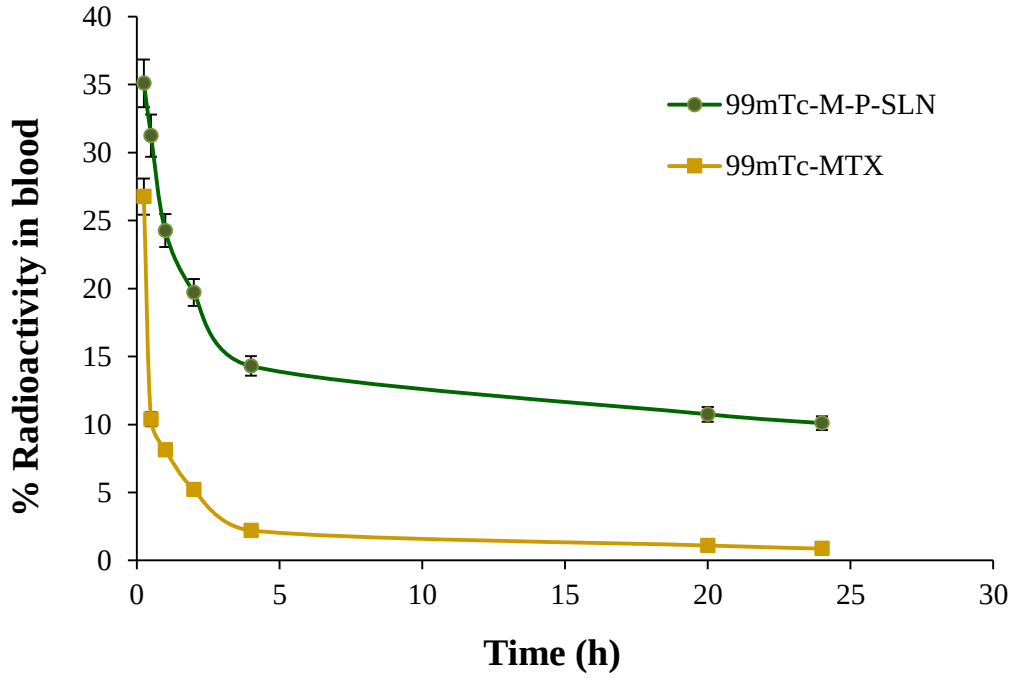

Fig 7: Blood clearance profile of ^{99m}Tc-MTX and ^{99m}Tc-M-P-SLNs over a period of 24h

99mTc-M-P-SLN 99mTc-MTX

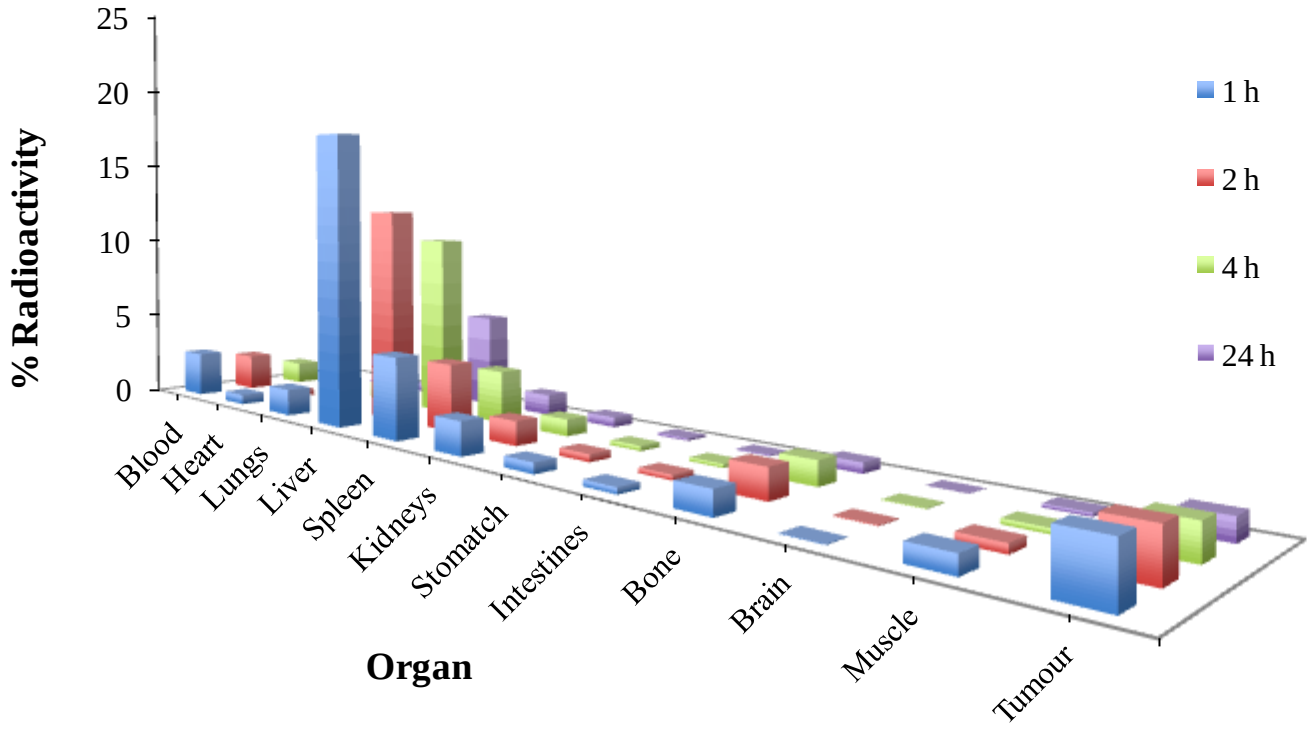

Fig 8: Biodistribution pattern of ^{99m}Tc-MTX loaded ^{99m}Tc-M-P-SLNs in tumour models(balb/c mice) over a period of 24h

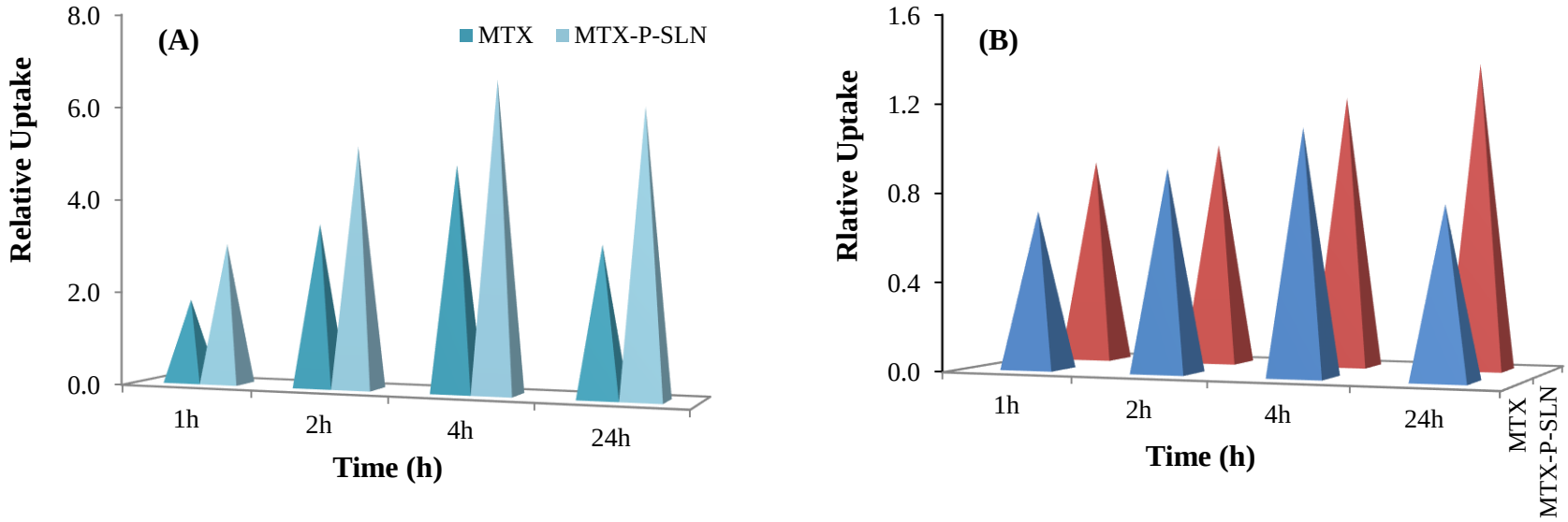

Fig 9: The relative uptake of ^{99m}Tc-MTX and ^{99m}Tc-M-P-SLNs (A) Tumour:muscle (B) Tumour:Blood, over a period of 24h

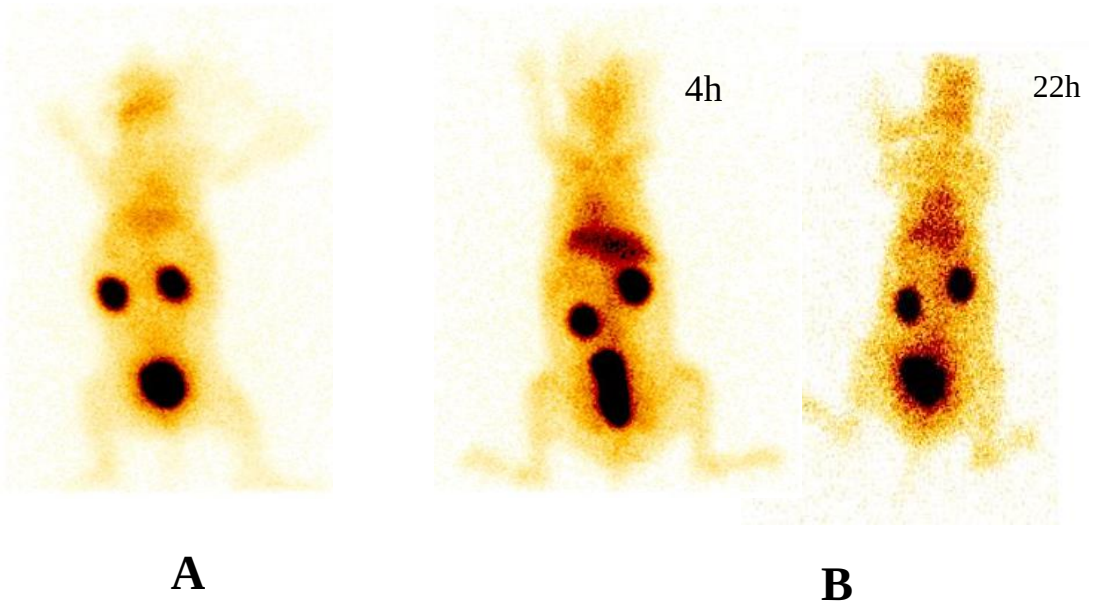

Fig 10: SPECT image of the in-vivo biodistribution of (A) ^{99m}Tc labeled MTX (at 4h p.i.) and (B) M-P-SA SLN formulation (at 4h and 22hp.i.) in new Zealand Albino rabbits

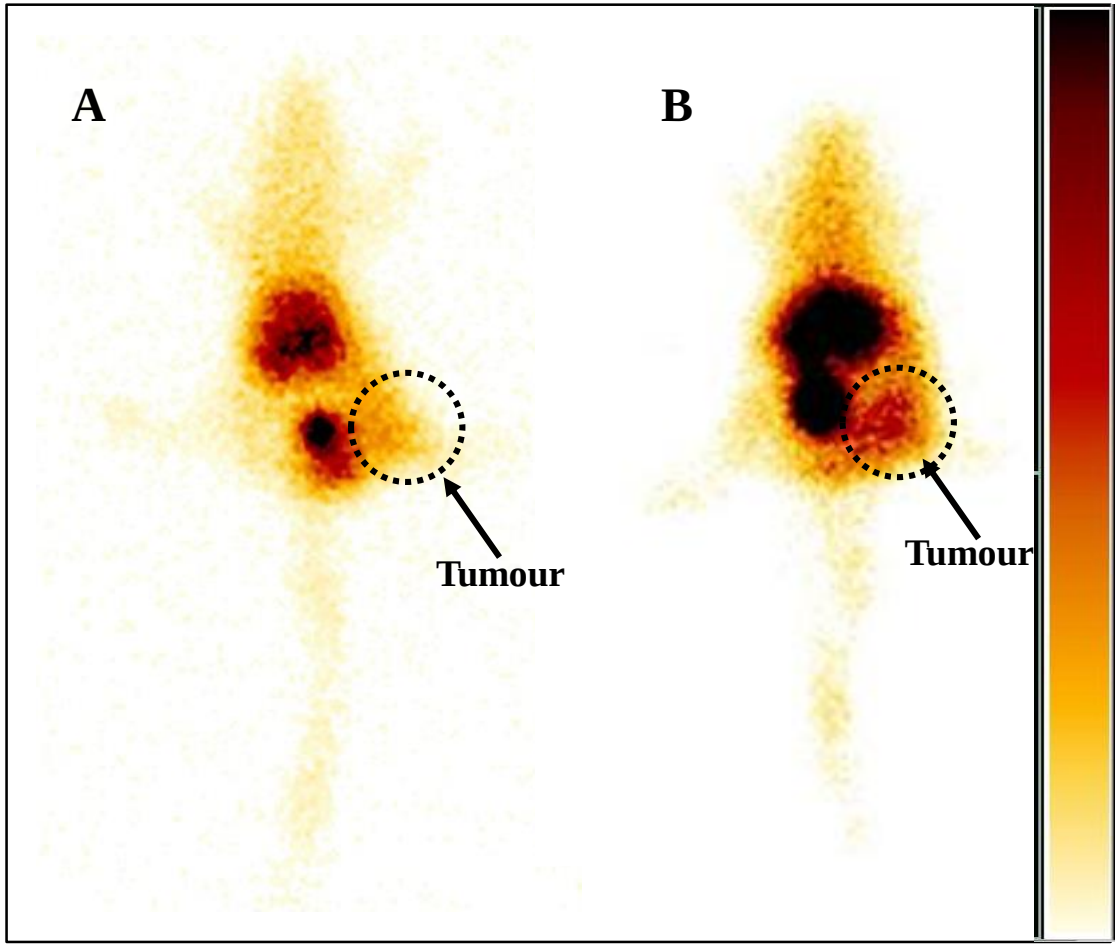

Fig 11: Whole-body γ-scintigraphic image of balb/c mice with subcutaneous EAT tumor at the right hind leg injected with (A)^{99m}Tc labeled MTX and (B) MTX-P-SLN formulation (4h p.i.)